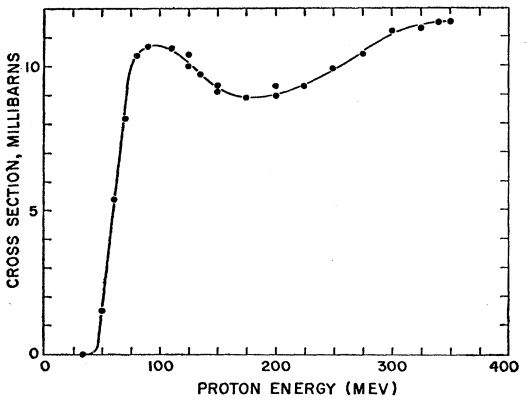

FIG. 2. Cross section of the reaction $Al^{27}(p,3pn)Na^{24}$.

Cross sections of the reaction $C^{12}(p,pn)C^{11}$ were obtained from the work of Crandall, Millburn, Pyle, and Birnbaum.[5] The results appear in Table I and Fig. 2.

III. DISCUSSION

The threshold of the reaction $Al^{27}(p,3pn)Na^{24}$ is calculated to be ~32 Mev if one disregards Coulomb barrier effects, and ~44 Mev if account is taken of the barrier. The cross section at 32 Mev was found to be 5×10^{-3} mb provided neutron background was negligible. This value disagrees with the value of ~0.5 mb given by Hintz and Ramsey.[1] The cross sections measured in this work from 50 to 125 Mev are consistently lower by about six millibarns than those of Hintz and Ramsey. The reaction $Al^{27}(p,pHe^3)Na^{24}$ has a threshold of 24 Mev if one disregards the Coulomb barrier, and one of 36 Mev if account is taken of the barrier. The present data indicate that the predominant reaction in the energy region studied is $Al^{27}(p,3pn)Na^{24}$.

IV. ACKNOWLEDGMENTS

The authors wish to thank Mr. Richard S. Gilbert for the use of his cross section at 32 Mev and for assistance in the measurement of the cross section at 350 Mev. We are also indebted to Dr. Wallace Birnbaum, Dr. Walter Crandall, Dr. George Millburn, and Dr. Robert Pyle for the use of their data[5] prior to publication. We wish to thank Mr. David Nethaway, Mrs. Joyce Gross, and Mrs. Therese Pionteki for assistance in counting the samples, and Mr. James Vale and the crew of the 184-inch cyclotron for conducting the bombardments.

PHYSICAL REVIEW VOLUME 102, NUMBER 5 JUNE 1, 1956

Pion Production by Inelastic Scattering of Electrons in Hydrogen*

W. K. H. PANOFSKY, W. M. WOODWARD,† AND G. B. YODH
High-Energy Physics Laboratory and Department of Physics, Stanford University, Stanford, California
(Received February 27, 1956)

The ratios of the yield of electron-induced to photon-induced pion processes have been measured at an incident energy of 600 Mev. Measurements have been made at energies of 60 and 170 Mev for positive pions. The result is expressed in terms of "the equivalent radiation length" X_e defined so that the pion yield due to direct electron production is equal to the pion yield due to photons produced by electrons in a radiator of X_e radiation lengths. The results are $X_e=0.0191\pm0.0011$ for 60-Mev pions and $X_e=0.0178\pm0.0023$ for 170-Mev pions. At the lower pion energy the value is somewhat lower than the theoretical value if equal transverse and longitudinal interactions are assumed. If the contribution from the longitudinal matrix element is taken to be small or if the electron contribution from large angles of electron scattering is suppressed, then the value can be fitted. The value at 170 Mev is in agreement with predominantly magnetic-dipole absorption corresponding to the enhanced $P_{3/2,3/2}$ state of the final pion-nucleon system.

I. INTRODUCTION

A. General

IN a previous paper,[1] we have discussed evidence for the direct production of positive pions by electron bombardment of lithium. Specifically, a measurement was carried out to establish the ratio of production by 500-Mev electrons to production by the corresponding photon bremsstrahlung of 60-Mev pions produced at 75° laboratory angle. Detailed interpretation of the lithium results is made difficult by the broadening effect of the initial momenta of the nucleons. For this reason, we have carried out further measurements using liquid hydrogen as a target. This paper covers measurements made only at one value of the incident electron energy (600 Mev), one pion laboratory production angle (75°), and two pion kinetic energies (60 and 170 Mev).

B. Kinematics and Description of the Process

Consider the inelastic collision between an electron and a proton resulting in pion formation. Figure 1 is a

* Supported in part by the joint program of the Office of Naval Research and the U. S. Atomic Energy Commission.
† On leave from the Laboratory for Nuclear Studies, Cornell University, Ithaca, New York.
[1] Panofsky, Newton, and Yodh, Phys. Rev. 98, 751 (1955).

vector momentum diagram for the kinematics of the process $e+p \rightarrow e'+n+\pi^+$. In this experiment the vectors $\mathbf{p}_1$ (initial electron energy) and $\mathbf{p}_\pi$ (pion momentum) are fixed. The final state will be completely defined provided the final electron angle is fixed. Since the final electron angle is not fixed in this experiment, the resultant cross section is an integral over the electron scattering angle. In principle, the pion and electron could be put in coincidence, but the experimental parameters make this impossible. It is, however, feasible to perform the complementary experiment to the one described here; namely, to observe the yield of inelastically-scattered electrons of given momentum corresponding to a cross section that is an integral over pion angles.

Figure 2 shows a family of curves of final electron momentum $|\mathbf{p}_2|$ as a function of electron scattering angle. Also plotted are the values of momentum transfer $|\Delta\mathbf{p}|$ and energy transfer Δp_0 to the meson-nucleon system. The momentum and energy transfers correspond exactly to the case of photon absorption for forward scattering of the electron only.

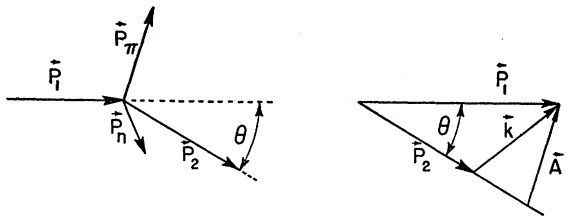

FIG. 1. Vector diagram representing the kinematics of pion production in electron-nucleon collisions, where $\mathbf{A}$ is the vector potential due to transition; $\mathbf{p}_1$ and $\mathbf{p}_2$ are the initial and final electron momenta; and $\mathbf{k}=\mathbf{p}_1-\mathbf{p}_2$ is the momentum of equivalent photon absorbed.

Photopion production and electron-pion production thus differ in the following respects: (1) In electron production the observed cross section is an integral over momentum transfer to the meson-nucleon system. (2) The vector potential corresponding to the "effective photon" field for electron scattering is transverse to the direction of momentum transfer only for zero scattering angle. The electron cross section thus includes contributions due to matrix elements (e.g., monopole, longitudinal electric dipole) that do not exist in photoproduction. (3) The various electromagnetic multipoles involved in pion production have a different dependence on the energy transfer and on the momentum transfer. Hence, the observed ratios of electron to photoproduction can give evidence either concerning the relative importance of the contribution of various multipoles, or, if this is assumed known,[2,3] concerning the behavior of the multipole matrix element as a function of momentum transfer, provided the contributions of the

[2] M. Gell-Mann and K. M. Watson, Ann. Revs. Nuclear Sci. 4, 219ff (1954).
[3] K. M. Watson (private communication).

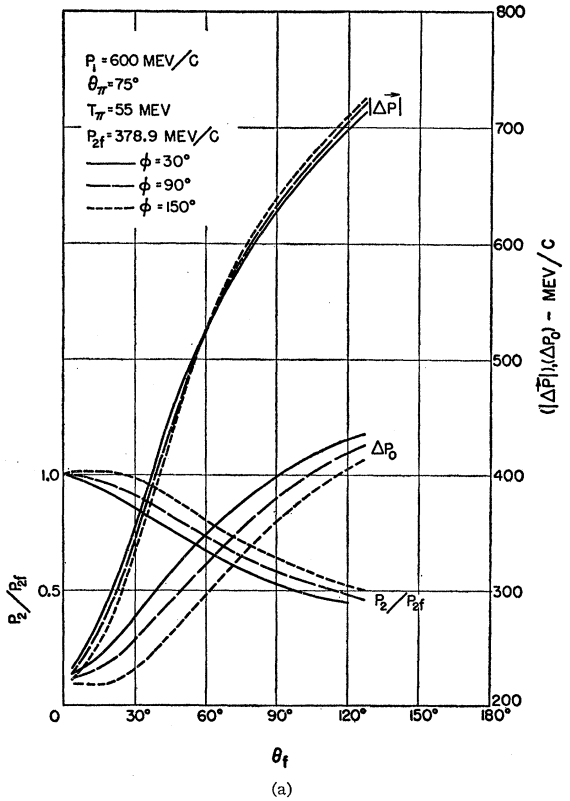

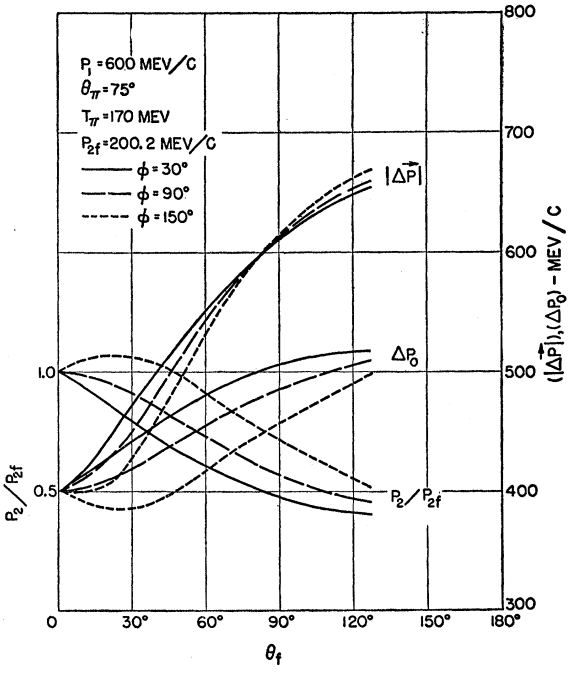

FIG. 2. Plots of momentum transfer ($|\Delta\mathbf{p}|$), energy transfer (Δp_0), and final electron energy as a function of final electron scattering angle; p_{2f} denotes the final electron momentum in the forward direction. Curves are shown for final pion energies of (a) 55 Mev and (b) 170 Mev; three different values of the azimuthal angle ϕ are used.

matrix elements not present in photoproduction are small. The latter can be interpreted in terms of a "form factor" of the matrix element in question, i.e., a factor indicative of a finite spatial extent of the interaction.

C. Definition of Measured Quantities

The experiment measures (1) the yield Y_k of mesons produced by absorption of a photon of momentum k corresponding to the fixed meson momentum, and (2) the yield Y_e of mesons produced by inelastic scattering of electrons with initial momentum p_1.

If $\sigma(k)$ is the differential photopion cross section; $N_k dk$ is the number of photons between k and $k+dk$; T_π is the pion kinetic energy; and N_0 is the number of protons per unit area of meson target; then

$$Y_k = N_0 \int (kN_k)\sigma(k)(dk/k). \tag{1}$$

Since the quantity (kN_k) is nearly equal to the radiator thickness X_R as measured in radiation lengths,

$$Y_k \approx N_0 \int X_R \sigma(k)(dk/k), \tag{2}$$

the yield Y_e is given by

$$Y_e = N_0 \int \sigma_e(E_0,E)dE, \tag{3}$$

where $\sigma_e(E_0,E)$ is the cross section for producing a meson by an electron of initial energy E_0 and final energy E. In the Weizäcker-Williams approximation, $\sigma_e(E_0,E)$ is related to $\sigma(k)$ via the virtual photon field.[4–6] We define a quantity N_e such that $N_e(dk/k)$ is the "number of virtual photons" between k and $k+dk$; then

$$Y_e = N_0 \int N_e \sigma(k)(dk/k). \tag{4}$$

In the Weizsäcker-Williams approximation,

$$N_e = (2\alpha/\pi)\ln(\gamma/kb_{\min}), \tag{5}$$

with symbols as defined in our previous paper.[1] The "equivalent" radiation length for electron production is then given in terms of N_e by

$$X_e = N_e/kN_k. \tag{6}$$

The equivalent radiation length is a number such that the meson yield due to photons from a radiator of thickness X_e equals the meson yield due to electrons directly.

[4] Nordheim, Nordheim, Oppenheimer, and Serber, Phys. Rev. 51, 1057 (1937).
[5] R. H. Dalitz and D. R. Yennie (to be published).
[6] For a discussion of the applicability of the Weizsäcker-Williams approximation, see references 1 and 5.

II. EXPERIMENTAL ARRANGEMENT

The experimental arrangement is the same as that described in our previous paper,[1] with the exception of the substitution of a liquid-hydrogen target for the solid-target arrangement used previously. Figure 3 shows the bombardment and meson-detection geometry. The liquid-hydrogen target is basically an aluminum cup of 0.002-in. wall, $5\frac{1}{2}$-in. long, 3-in. wide, and 7-in. high. The cup is surrounded by a layer of Styrofoam, a liquid-nitrogen jacket, and a second layer of Styrofoam. The nitrogen jacket is designed with large windows at the points of entry and exit of the electron beam.

In this experiment, it is necessary to minimize a quantity X_j which measures the radiation length of radiating material in the path of the electron beam in the absence of an intended radiator; X_j is measured in equivalent radiation lengths of copper. The exit window of the accelerator, the intervening air space, Styrofoam and aluminum layers, and the liquid hydrogen itself contribute to X_j. The contribution from the hydrogen is more difficult to determine since it depends on the efficiency of meson detection as a function of the distance x along the beam. To measure this contribution, the following procedure was adopted: The pion detection efficiency profile $f(x)$ was determined experimentally by plotting pion counts as a function of x with a thin copper target placed at x. The coordinate x of the copper target along the beam was read with a telescope traveling on a horizontal precision vernier caliper. Curves of $f(x)$ for each of the runs described here are shown in Fig. 4. Let $\bar{x} = \int x f(x)dx / \int f(x)dx$. The contribution X_{Hj} of the hydrogen to X_j can then be shown to be

$$X_{Hj} = \bar{x}_{g/cm^2} N_A k \sigma_H(k)/(kN_k)_{copper}, \tag{7}$$

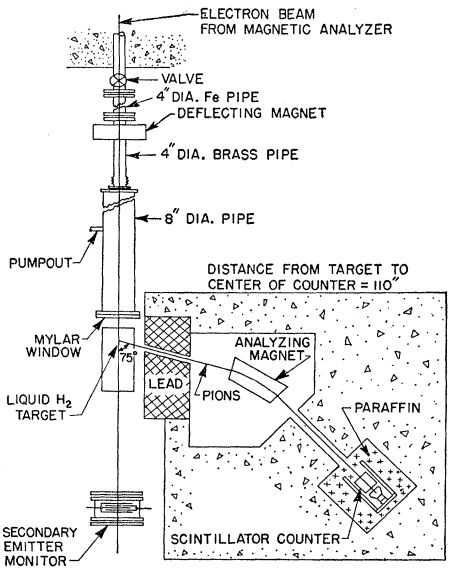

FIG. 3. Meson detection geometry.

where N_A is Avogadro's number; $\sigma_H(k)$ is the differential radiation cross section in hydrogen; and $(kN_k)_{\text{copper}}$ measures the product of photon energy times photon number per unit radiation length of a copper radiator (as discussed above, this number is nearly equal to unity).

The zero of x in evaluating the integrals of the "acceptance profiles" must be chosen to conform to the edge of the hydrogen cup in the target. This can be achieved by locating the target with the same telescope arrangement used in defining the abscissas of $f(x)$; a window in the hydrogen target permits observation of the leading edge of the target.

The differential cross section σ_H has been measured in a separate experiment[7] and is found to be lower than the theoretical value calculated by Wheeler and Lamb[8] by $(2.9\pm2.8)\%$. The calculation of Wheeler and Lamb omits exchange terms and uses atomic rather than molecular wave functions for the screening calculations in the radiation from electron-electron collisions. The experimental value has been used in calculating X_e.

III. PROCEDURE

The experimental arrangement permits the pion yield to be measured under the conditions listed in Table I. We shall denote counts taken with the radiator in and the target empty by C^{+-}; with the radiator out and the target full by C^{-+}; and so forth. We shall use the subscript d for data taken with the beam deflected down.[9] Let us define quantities A and B such that

$$A=X_j+X_e\propto C^{-+}-C^{--}-(C_d{}^{-+}-C_d{}^{--}), \quad (8)$$

$$B=X_R+X_j+X_e\propto C^{++}-C^{+-}-(C_d{}^{++}-C_d{}^{+-}), \quad (9)$$

where X_R is the radiator thickness in radiation lengths. The counts C^{--} and C^{+-} represent the empty-target counts and are thus background counts due to neutrons and other background effects. The differences $(C_d{}^{-+}-C_d{}^{--})$ and $(C_d{}^{++}-C_d{}^{+-})$ represent possible counts due to gamma-ray or neutron admixture in the primary beam. In practice, this latter correction is small and is not in fact statistically significant. The quantity A thus represents the observed corrected count without radiator, and B the observed corrected count with radiator; X_e is then calculated from the relation

$$X_e=\frac{X_R}{[(B/A)-1]}-X_j. \quad (10)$$

Equations (8) and (9) assume that the presence of liquid hydrogen does not affect the background appreciably. The principal reason for background after the beam pulse is due to moderated neutrons, which produce delayed pulses by their capture radiation. Hydrogen contributes to the neutron production via the photopion cross section. The magnitude of this effect has been estimated and found to contribute an error of less than $\frac{1}{2}\%$ to the calculated values of N_e. The estimate is performed as follows: The difference $(C^{+-}-C^{--})$ represents the neutron background from the radiator; the neutron background from the hydrogen is then estimated from the known cross section ratio of photonuclear neutron production (the process important for neutron production in the radiator) to the photopion cross section (the process important for the neutron yield from hydrogen). The reason for the small contribution is the fact that the neutron contribution resulting from pion production would vary essentially proportionately to the observed pion yields C^{++} and C^{-+}, respectively; since N_e depends on the ratios of the counts C^{++} to C^{-+}, this potential background variation has a very small effect on N_e.

Counts were taken with reference to two secondary-electron monitors as described previously.[1,10] Both instruments were placed beyond the hydrogen target in order to avoid contributing to the value of X_j. We have to assume, of course, that the monitor readings

TABLE I. Experimental conditions under which the pion yield was measured.

Radiator	In	Out
Hydrogen target	Full	Empty
Beam	Straight	Deflected down

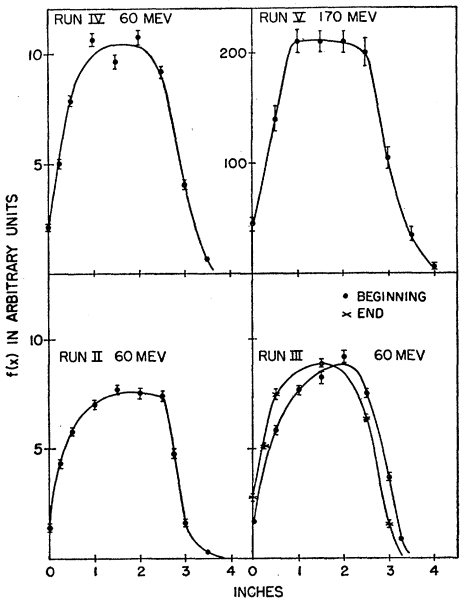

FIG. 4. The pion detection efficiency profiles $f(x)$, where x is the position coordinate along the electron beam, and $x=0$ corresponds to the front edge of the liquid hydrogen.

[7] D. Bernstein and W. K. H. Panofsky, Phys. Rev. **102**, 522 (1956).
[8] J. A. Wheeler and W. E. Lamb, Phys. Rev. **55**, 858 (1939).
[9] For details of the deflecting-down process, see reference 1.
[10] G. W. Tautfest and H. R. Fechter, Rev. Sci. Instr. **26**, 229 (1955).

TABLE II. Summary of the experimental data. X_{Hj} and X_j are the radiation lengths of hydrogen and of remaining material, respectively, in the electron beam.

Run	C^{++}	C^{+-}	C^{-+}	C^{--}	Cd^{-+}	Cd^{--}	X_{Hj}	X_j	T_π (Mev)
I	6.98 ±0.108	0.203±0.14	3.026±0.093	0.117 ±0.011	0.233±0.016	0.117±0.117[a]	0.00397	0.01092±0.00063	60
II	10.54 ±0.206	0.108±0.035	4.548±0.0674	0.140 ±0.033	0.295±0.04	0.304±0.066	0.00358	0.00705±0.00044	60
III	6.851±0.136	0.24 ±0.035	3.057±0.0457	0.13 ±0.025	0.16 ±0.06	0.08 ±0.08[a]	0.00401	0.00748±0.00045	60
IV	2.388±0.0743	0.163±0.023	1.098±0.0277	0.0705±0.015	0.32 ±0.067	0.19 ±0.44	0.00529	0.00890±0.00046	170

[a] Here the Cd^{--} background was not taken; the numbers used are conservative estimates taken as $[(Cd^{-+}/2)\pm(Cd^{-+}/2)]$.

were not affected by the introduction of the liquid hydrogen. This was established in connection with a separate experiment.[11] The results indicate that monitoring is affected to an extent <0.5% by the introduction of the target.

The primary beam energy was defined by the energy acceptance of the beam-analyzing system of the linear accelerator.[12] The system in turn was calibrated using the floating-wire technique. With this method the selected energy is standardized against the magnet current. Although the method is sensitive to within better than 1%, the uncertainty of some of the primary-energy values used in the early runs may be in error as much as 5% due to uncertainty in the current shunts used.

The energy of the pion was determined either by the momentum acceptance of the magnet analyzing system or by the range definition of the pions. For the runs at 60 Mev no absorbers other than the plastic scintillator detector (10 in. deep) defined the range; hence in general the momentum channel defined the energy. The momentum channel was calibrated by the floating-wire technique. In some of the runs there was evidence, however, that nonuniform light collection in the scintillator may have biased the energy value. We believe that the energy value at the 60-Mev pion energy is correct to ±10 Mev.

The run at high pion energy was performed by placing a copper absorber (22.6 g/cm²) ahead of the magnetic analyzer, and a second absorber (28.3 g/cm²) after the analyzer and ahead of the counter. Under this condition the energy was defined by the sensitive range interval in the scintillator and not by the magnet parameters. The energy value was checked in a separate experiment by observing the yield of pions as a function of beam energy using a polyethylene-carbon subtraction method. The result corresponds to $T_\pi = 170\pm15$ Mev for the parameters used (Fig. 5).

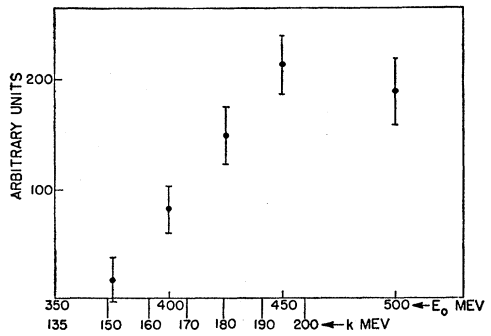

FIG. 5. Excitation function for 170-Mev pions from hydrogen. pion energy uncertainty is estimated from the curve to be ±15 Mev.

IV. RESULTS

The results of four series of runs are shown in Table II. Results are expressed as counts per 10^{-7} coulomb of electron bombardment as observed by the monitor. The absolute counts per incident electron are not constant from run to run since the values of the counter efficiencies were not re-established to the same value between runs. During each run counts of the various types were alternated to minimize the effect of possible gain instabilities.

We have assigned standard deviations to the computed values as tabulated above both as a result of the counting statistics and of the estimated precision of the auxiliary measurements. Among these we have included: (1) uncertainty in the evaluation of $f(x)$: ±0.1 in. in the value of $\bar{x}$, corresponding to ±2.0% in X_e; (2) uncertainty in the radiator thickness: ±1.0%, corresponding to ±1.5% in X_e; (3) uncertainty in X_j due to the local variability of the Styrofoam density: ±6% in density, corresponding to ±1.2% (Run I) and to ±0.4% in Runs II–IV in the value of X_e. We believe that errors due to monitoring and drifts in counting efficiency are negligible due to the procedure of alternating the types of counts.

In reducing the data from Table II to yield values of X_e and N_e, we have used auxiliary constants given in Table III. The values were computed for an incident energy of 600 Mev from the Bethe-Heitler formula in intermediate screening.[13] An additional correction of −1.3% was made to the value of $(kN_k)_{\text{copper}}$ from the Bethe-Heitler formula to account for the observed[11] and theoretical[14] deviation from the Born approximation. From these data, we obtained the values contained in Table IV; the values of X_e (equivalent radiation length) and N_e (number of virtual photons) are related by (kN_k) where N_k describes the photon spectrum from the radiator (Fig. 6).

[11] K. L. Brown (to be published).

[12] W. K. H. Panofsky and J. A. McIntyre, Rev. Sci. Instr. **25**, 287 (1954).

[13] H. A. Bethe and J. Ashkin, *Experimental Nuclear Physics*, edited by E. Segrè (John Wiley and Sons, Inc., New York, 1953), Vol. I, pp. 259 ff.

[14] H. Olsen, Phys. Rev. **99**, 1335 (1955).

V. DISCUSSION

Interpretation of the results is complicated by the fact that for the measurements at $T_\pi=60$ Mev, there might be an appreciable contribution from multiple pion production; i.e., π^+ mesons from the processes $\gamma+p\rightarrow p+\pi^++\pi^-$; $\gamma+p\rightarrow n+\pi^++\pi^0$; and $e+p\rightarrow p+e'+\pi^++\pi^-$; $e+p\rightarrow n+e'+\pi^++\pi^0$. We can demonstrate, however, that we can take account of this possibility without a substantial increase in the uncertainty of the result.

The threshold for the electron-pion pair process corresponds to a recoil electron momentum of $p_2=190$ Mev/c. Since the electron-pion pair-production process has a four-body final state, p_2 is not unique even if it is assumed that p_2 is directed along the forward direction. For pion-pair production, $X_{e(\text{pair})}$ is calculated by averaging over all allowed values of $k=p_1-p_2$. It is sufficient for our purposes to assume (1) that the variation of the cross section for pair production with energy is given solely by the density of the final states, and (2) that p_2 is directed along the forward direction.

Fortunately, it is true in general that if $p_2\ll p_1$, the detailed value of $X_{e(\text{pair})}$ is insensitive to detailed considerations. We can therefore correct for the presence of the pair process to sufficient accuracy without either detailed theoretical analysis of $X_{e(\text{pair})}$ or exact experimental information on the cross section for the photopion pair processes.

TABLE III. Radiation length in copper $(kN_k)_{\text{copper}}$ for given pion energies, and the thickness t of the radiator used in radiation lengths of copper.

T_π	$(kN_k)_{\text{copper}}$	X (g/cm²)	t (radiation lengths)
60 Mev (Runs I–III)	0.967	0.458	0.0359
170 Mev (Run IV)	0.869	0.448	0.0352

We estimate the photopion pair contribution on the basis of the work of Crowe, Friedman, and Motz[15] now in progress at this laboratory. Crowe *et al.* measure the pair process by two methods: (a) by observing the yield of negative photopions from hydrogen, and (b) by observing the variation of the yield of positive photopions of fixed energy and angle with the upper limit of the bremsstrahlung spectrum used. Results from the second method are most useful for our purpose, since positive pions are observed directly, and since the contribution from both $(\pi^+\pi^-)$ and $(\pi^+\pi^0)$ pairs is included. On the basis of their work we estimate that a fraction $f=(15\pm4)\%$ of the positive mesons observed in our measurement at $T_{\pi^+}=60$ Mev and a laboratory angle of 75° are pair fragments from double photopion production.

[15] Crowe, Friedman, and Motz (private communication),

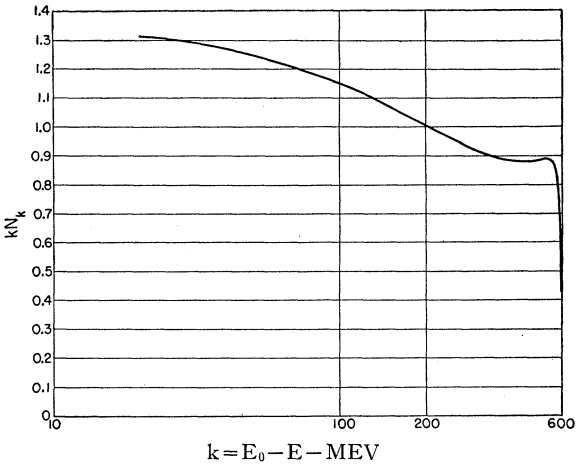

FIG. 6. Variation of $(kN_k)_{\text{copper}}$ with k calculated in Born approximation (see reference 13). The actual value of $(kN_k)_{\text{copper}}$ is lower by 1.3% in the complete-screening region. E_0 is initial electron energy and E is final electron energy.

The total range of variation of the calculated value of X_e over the interval for p_2 indicated above is only $0.011<X_e<0.017$. If we perform the integration over the excitation of the pion pair process using the phase space factor only, we obtain $X_{e(\text{pair})}=0.014$; we can safely take $X_{e(\text{pair})}=0.014\pm0.002$. Hence the observed value of X_e becomes

$$X_e=(1-f)X_{e(\text{single})}+fX_{e(\text{pair})}. \tag{11}$$

The correction is thus $(4.5\pm2)\%$. As a result of this calculation, we obtain

$$X_{e(\text{single})}=0.0200\pm0.0011,$$
$$N_{e(\text{single})}=0.0193\pm0.0010,$$

for $T_\pi=60$ Mev. The values for $T_\pi=170$ Mev remain $X_e=0.0178\pm0.0023$ and $N_e=0.0155\pm0.0020$.

Detailed predictions concerning the electron cross section as affected by the various parameters of photopion production are discussed by Dalitz and Yennie.[5] The value of N_e represents an integral of the inelastic-scattering cross section over the electron scattering angle Most of the contribution comes from forward angles; it is clear however, that in the limit of zero scattering angle there will be an exact correspondence

TABLE IV. Measured values of X_e and N_e for $T_\pi=60$ Mev and $T_\pi=170$ Mev, $\theta_\pi=75°$ (laboratory), and 600-Mev electrons. Quoted errors in Runs II–IV are the statistical errors computed from the total counts. Quoted errors in I are based on internal consistency as computed from scatter of individual counts.

Run	T_π (Mev)	X_e	$\bar{X}_e$	N_e
I	60	0.01505 ± 0.00332	0.01910 ± 0.0011	0.0185 ± 0.0010
II	60	0.01923 ± 0.00133		
III	60	0.02001 ± 0.00190		
IV	170	0.0178 ± 0.0023	0.0178 ± 0.0023	0.0155 ± 0.0020

TABLE V. Theoretical values for X_e calculated assuming different matrix elements for $T_\pi=60$ Mev and $T_\pi=170$ Mev, and 600-Mev electrons.

Case	$T_\pi=60$ Mev	$T_\pi=170$ Mev
(i)	0.0203	0.0172
(ii)	0.0218	0.0176
(iii)	0.0243	0.0188

of photon production and electron production; hence, identification of effects giving results beyond those known from photopion production requires considerable accuracy. In the work described here, sufficient accuracy to indicate results beyond those known from the corresponding photopion production has been attained in respect to only one result: namely, our estimate concerning the relative magnitude of the longitudinal and transverse components of the electric-dipole matrix element.

The variables affecting the value of N_e can be summarized as follows: (1) the type of multipole effective in the pion-production process at the pion energy and angle chosen; (2) the behavior of the predominant multipole matrix elements as a function of momentum transfer; this behavior can be characterized phenomenologically by a form factor corresponding to a finite spatial extent of the interaction; (3) the contribution of matrix elements not possible for a photon field, namely, longitudinal electric dipole matrix elements and "monopole" (i.e., purely radial) interaction.

In particular, we shall compare the experimental values with the theoretical values in three cases (Table V): (i) pure electric-dipole absorption, longitudinal matrix element absent; (ii) pure electric-dipole absorption, longitudinal and transverse matrix elements equal;[16] (iii) magnetic-dipole absorption. The 60-Mev experimental value is certainly significantly below (ii) and (iii). Since analysis of the photopion process[3] attributes the cross section at 60 Mev predominantly to electric-dipole absorption, it is clear that the longitudinal matrix element is probably small.

The observed value at 170 Mev is in fair agreement with the theoretical value expected for pure magnetic-dipole interaction. Such an interaction corresponds to the final meson-nucleon system in the $P_{3/2,3/2}$ state. The precision of the experiment is not sufficient to draw any inference as to the possible contribution of a finite spatial extent interaction.

VI. ACKNOWLEDGMENTS

This experiment has been aided materially by many members of this laboratory. The experimental equipment used evolved from the contributions primarily of Dr. K. M. Crowe, and also of Dr. J. A. Narud, C. M. Newton, R. M. Friedman, S. W. Lee, and others. We are particularly indebted to the linear accelerator operating group, under Professor R. F. Mozley, for providing a beam under frequently difficult operating conditions; in particular, the efforts of R. G. Gilbert in this connection are greatly appreciated. We are indebted to Dr. K. L. Brown, P. D. Toft, D. M. Bernstein, and Dr. G. E. Masek for assistance during the runs.

Our theoretical understanding of this problem has been derived primarily from discussion with Professor R. H. Dalitz and Professor D. R. Yennie; their contribution is gratefully acknowledged.

[16] This is the case called "electric dipole" by J. S. Blair, Phys. Rev. **75**, 907 (1948); mineographed notes; and private communications to Richard Wilson and K. L. Brown; and by Thie, Mullin, and Guth, Phys. Rev. **87**, 962 (1952).